2013 European Control Conference (ECC)
July 17-19, 2013, Zürich, Switzerland.

Inverse signal shapers in effective feedback architecture

Tomáš Vyhlídal[1], Martin Hromčík[2], Vladimír Kučera[1]

Abstract— **New feedback control architecture is proposed in this paper suitable for manipulation of weakly damped flexible structures. Delay-based signal shapers are considered since they are very popular in such applications for their simple implementation and very good performance. Unlike the classical approach where the shapers are used just to filter the reference command, we consider placing it inside the closed loop. Compared to previous attempts, we propose to include the inverse of the signal shaper's dynamics in the feedback path. This architecture is justified by thorough analysis of important feedback loop channels, namely the feedback response from input disturbance to the output. As results from the spectral properties, classical ZV shapers with lumped delays are very inconvenient for the shaper inverse operation, leading to neutrality of the dynamics with the associated risks of stability loss due to high frequency unstable modes. Therefore, a recently introduced DZV shaper with a distributed delay element is utilized in the feedback loop. Results are verified by simulations and experiments.**

I. INTRODUCTION

The long tradition in signal shaping using time delay elements started in 1950's [12] [14]. Subsequently, in the 1990's, the subject was extensively studied by Singer and Seering [16]. They proposed the concepts of zero-vibration-derivative (ZVD) and extra insensitive (EI) shapers. Since then, many modifications of the shapers have been proposed, and various aspects concerning the properties of the shapers have been studied, e.g. parameter adaptation in [10], [9], discrete shaper implementation in [20], [7], [1], and robustness analysis in [15], [21].

Next to the feed-forward shaper-system interconnection, strong attempts to incorporate signal shapers directly into feedback interconnections, positioning servomechanisms for flexible systems as an example, can be identified. Such an arrangement should handle in principle not only the effect of the reference command (always known, or measurable), but also the effect of unmeasurable disturbances to the excitation of the flexible modes. Smith in [13] and later Hung in [6] proposed a straightforward augmentation of the standard feedback loop with pre-tuned input command shaper. Closed loop stability issues related to signal shapers placed inside feedback connections are discussed by Huey and Singhose in [4] using simple root locus diagrams, and by Staehlin and Singh in [18]. From the available literature, however, it can be concluded that the signal shaper being placed in the loop between the controller and the system is rather ineffective in the given objective of suppressing the vibrations caused by disturbance variables. For example, in [5], it is shown that the architecture is effective in suppressing the sensor disturbances, but completely ineffective in suppressing the oscillations themselves as they are excited by the disturbance.

The main motivation of the presented paper is to design a closed loop architecture with the shaper, which is effective in suppressing the vibrations from both the set-point adjustments and the disturbances. The paper is organized as follows. In Section II and III, the problem definition and the preliminaries in the given signal shaping subject are given. The main results are presented in section IV, where the novel architecture with the shaper is proposed. It is followed by sections V and VI on simulation and experimental validation and by brief concluding section VII.

II. PROBLEM FORMULATION

Consider the objective to suppress oscillatory dynamics of a flexible part of a system in the set-up shown in Fig. 1. As can be seen, it consist of two parts, System 1 with the transfer function $G(s) = \frac{x(s)}{u(s)} = \frac{M(s)}{N(s)}$, where u, x are the system input and output, respectively, and System 2, the flexible part, with transfer function $F(s) = \frac{y(s)}{z(s)} = \frac{L(s)}{H(s)}$, where y is the system output and $z = d+x$ is its input, where d is unmeasurable disturbance. $M(s), N(s), L(s), H(s)$ are polynomials with degrees m, n, b, a. We consider $G(s)$ being strictly proper, i.e. $m < n$, and $F(s)$ being proper at least, i.e. $b \leq a$.

Let the oscillatory mode of System 2 to be compensated by the shaper is represented by the natural frequency ω_0 and the damping ratio ζ, determining the complex conjugate couple of poles $r_{1,2} = -\beta \pm j\Omega, \beta = \omega_0\zeta, \Omega = \omega_0\sqrt{1-\zeta^2}$ of transfer function $F(s)$, i.e., the roots of polynomial $H(s)$.

III. PRELIMINARIES

A. Signal shapers

For the oscillatory mode compensation purpose, we can use the simple ZV shaper [15], [16], in serial connection with the system, as shown in Fig. 1, given by

$$u(t) = Aw(t) + (1-A)w(t-\tau), \tag{1}$$

where w and u are the shaper input and output, respectively. The parameters are the gain $A \in [0.5, 1)$ and the time delay $\tau \in \mathbb{R}^+$.

The presented research results were supported by The Technology Agency of the Czech Republic under the Competence Centre Project TE01020197, Centre for Applied Cybernetics 3 (authors[1]) and by the Czech Science Foundation (GACR) under the contract No. 13-06962S (author[2])

[1]T. Vyhlídal and V. Kučera are with the Department of Instrumentation and Control Engineering, Faculty of Mechanical Engineering, Czech Technical University in Prague, Technicka 4, Prague 6, Czech Republic. tomas.vyhlidal@fs.cvut.cz, vladimir.kucera@fs.cvut.cz

[2]M. Hromčík is with Department of Control Engineering, Faculty of Electrical Engineering, Czech Technical University in Prague, Karlovo namesti 13, Prague 2, Czech Republic. xhromcik@fel.cvut.cz

The zeros of shaper (1) are determined by the roots of the equation

$$S_{ZV}(s) = A + (1-A)e^{-s\tau} = 0, \tag{2}$$

which are given as follows

$$s_{2k+1,2k+2} = -\frac{1}{\tau}\ln\frac{A}{1-A} \pm j\frac{\pi}{\tau}(2k+1), k = 0, 1, ..., \infty. \tag{3}$$

From these infinitely many zeros, only the dominant pair $s_{1,2} = -\frac{1}{\tau}\ln\frac{A}{1-A} \pm j\frac{\pi}{\tau}$ is used in fact to compensate the pole of the system $r_{1,2}$ [12], [4]. Placing the dominant zero $s_{1,2}$ of (1) at the position of $r_{1,2}$, the parameters of the shaper are given as follows

$$A = \frac{e^{\frac{\beta}{\Omega}\pi}}{1+e^{\frac{\beta}{\Omega}\pi}}, \tau = \frac{\pi}{\Omega}. \tag{4}$$

In [24], [23], as an alternative to ZV shaper, the shaper with equally distributed delay (DZV shaper) has been proposed as

$$u(t) = Bw(t) + \frac{(1-B)}{\vartheta}\int_0^{\vartheta} w(t-\eta)d\eta, \tag{5}$$

where w and u are the shaper input and output, respectively, $B \in \mathbb{R}^+, B < 1$ is the gain parameter, and the delay is equally distributed over the interval $[0, \vartheta]$. As shown in [24], the transfer function of the shaper (5) is given by

$$S_{DZV}(s) = B + (1-B)\frac{1-e^{-s\vartheta}}{s\vartheta} \tag{6}$$

The spectrum of zeros of (6), i.e. solutions of equation $S_{DZV}(s) = 0$, can be determined as the nonzero roots of the following equation

$$B\vartheta s + (1-B)(1-e^{-s\vartheta}) = 0. \tag{7}$$

The infinite spectrum of the transcendental equation (7) is given by

$$\begin{gathered} s_k = \frac{1}{\tau}\left(W\left(k, \frac{1-B}{B}e^{\frac{1-B}{B}}\right) - \frac{1-B}{B}\right), \\ k = -\infty..., -2, -1, 0, 1, 2, ...\infty. \end{gathered} \tag{8}$$

where W is the Lambert W function [25]. From the infinitely many complex conjugate roots, the roots $s_{-1,1}$ corresponding to $W(-1, \cdot)$ and $W(1, \cdot)$, respectively, are to be used to compensate the oscillatory mode of the system given by $r_{1,2} = -\beta \pm j\Omega$. As shown in [24], [23], the parameter ϑ is given by the smallest positive real root of the following quasi-polynomial equation

$$\Omega e^{-\beta\vartheta} + \beta sin(\Omega\vartheta) - \Omega cos(\Omega\vartheta) = 0, \tag{9}$$

which lies within the interval $(\frac{\pi}{\Omega}, \frac{2\pi}{\Omega})$. Consequently, the parameter B is given by

$$B = \frac{sin(\Omega\vartheta)}{sin(\Omega\vartheta) - \vartheta\Omega e^{\beta\vartheta}}. \tag{10}$$

In [24] and [23], the comparison of various characteristics of ZV and DZV shapers have been performed. From the comparison of time domain characteristics it results that for $\zeta = 0$, the time response of the DZV shaper is twice as long as the response of the ZV shaper. However, as ζ increases, the difference between the response duration decreases. From the comparison of the residual sensitivity functions performed in [24] and [23], it results that the DZV shaper has considerably better robustness features at higher frequency range compared to the classical ZV shaper. Besides, spectrum of DZV shaper is retarded, whereas the spectrum of ZV shaper is neutral.

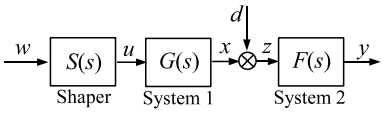

Fig. 1. Open loop system with signal shaper

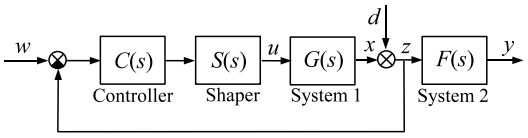

Fig. 2. Closed loop system with signal shaper

B. Shaper in the closed loop

With a shaper placed in the open loop as in Fig. 1 only the oscillations induced by the system control input can be compensated. Obviously, the shaper cannot compensate the oscillations induced by the system disturbance d. A natural option to improve the shaper performance in this task is to close a feedback loop as shown in Fig. 2, with a controller $C(s) = \frac{P(s)}{Q(s)}$, where $P(s), Q(s)$ are polynomials with degrees p, q, $p \leq q$. This control scheme has for example been considered in [6], [4], [11], [5]. However, as it can easily be seen from the transfer functions of the closed loop system

$$\begin{aligned} T_{wy}(s) = T_{wz}(s)F(s) = \frac{C(s)G(s)S(s)}{1+C(s)G(s)S(s)}F(s) = \\ = \frac{P(s)M(s)S(s)}{Q(s)N(s)+P(s)S(s)M(s)}\frac{L(s)}{H(s)}. \end{aligned} \tag{11}$$

$$\begin{aligned} T_{dy}(s) = T_{dz}(s)F(s) = \frac{1}{1+C(s)G(s)S(s)}F(s) = \\ = \frac{Q(s)N(s)}{Q(s)N(s)+P(s)S(s)M(s)}\frac{L(s)}{H(s)}, \end{aligned} \tag{12}$$

the desirable mode compensation can take place only for $T_{wy}(s)$. In this case, the active zeros of the shaper $S(s)$ are the zeros of the closed loop system, given as the solutions of the following equation

$$P(s)M(s)S(s) = 0. \tag{13}$$

Thus, the dominant zeros of $S(s)$ can compensate the pole $r_{1,2}$ of $F(s)$. However, in $T_{dy}(s)$, the shaper transfer function $S(s)$ does not appear in the numerator of the closed loop system. Therefore the zeros of the shaper are not the zeros of the closed loop system, given by the roots of the equation

$$Q(s)N(s) = 0, \tag{14}$$

as also pointed out in [5].

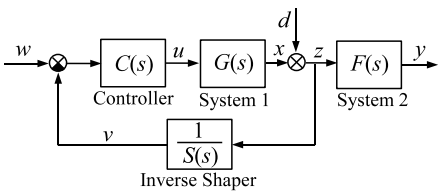

Fig. 3. Closed loop system with inverse signal shaper

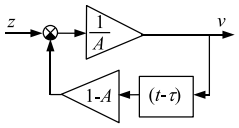

Fig. 4. Implementation of inverse ZV shaper

Thus, the shaper in the loop suppresses only the oscillations induced by the reference w whereas it is entirely ineffective in suppressing the oscillations induced by the disturbance d. In fact, with respect to the suppression of the oscillatory mode of system $F(s)$, the schemes in Fig. 1 and Fig. 2 are equally efficient.

IV. Main result - inverse shaper in the feedback loop

As the main result, we propose a new closed loop architecture with an inversion of the shaper shown in Fig. 3. The main advantage of this novel scheme can directly be seen from the transfer functions

$$\begin{aligned} T_{wy}(s) = T_{wz}(s)F(s) = \frac{C(s)G(s)}{1+C(s)G(s)\frac{1}{S(s)}}F(s) = \\ = \frac{P(s)M(s)S(s)}{S(s)Q(s)N(s)+P(s)M(s)}\frac{L(s)}{H(s)}, \end{aligned} \tag{15}$$

$$\begin{aligned} T_{dy}(s) = T_{dz}(s)F(s) = \frac{1}{1+C(s)G(s)\frac{1}{S(s)}}F(s) = \\ = \frac{Q(s)N(s)S(s)}{S(s)Q(s)N(s)+P(s)M(s)}\frac{L(s)}{H(s)}, \end{aligned} \tag{16}$$

where the shaper transfer functions $S(s)$ appears in numerator of both the closed loop transfer functions. Thus, the shaper can compensate the oscillatory mode induced by both the set-point w and the disturbance d. However, as will be shown, the novel scheme in Fig. 3 can bring about negative consequences on closed loop dynamics, especially if the ZV shaper is applied. Before the closed loop dynamics analysis, let the inverse implementation of the shapers be introduced.

A. Inverse shaper implementation

For the application of the shaper in the inverse form, the transfer function of the zero vibration shapers are given as

$$\frac{1}{S_{ZV}(s)} = \frac{v(s)}{z(s)} = \frac{1}{A+(1-A)e^{-s\tau}}, \tag{17}$$

for inverse ZV, and

$$\frac{1}{S_{DZV}(s)} = \frac{v(s)}{z(s)} = \frac{1}{B+(1-B)\frac{1-e^{-s\vartheta}}{s\vartheta}}, \tag{18}$$

for inverse DZV shapers. In time domain, the ZV shaper is given by

$$v(t) = \frac{1}{A}\left(z(t) - (1-A)v(t-\tau)\right), \tag{19}$$

and the DZV shaper is given as follows

$$v(t) = \frac{1}{B}\left(z(t) - \frac{(1-B)}{\vartheta}\int_0^{\vartheta} v(t-\eta)d\eta\right). \tag{20}$$

In Fig. 4 and Fig. 5 the implementation schemes of both the inverse shapers are shown.

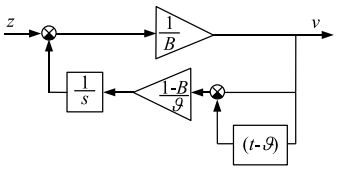

Fig. 5. Implementation of inverse DZV shaper

B. Dynamics analysis of the closed loop system

The spectra of zeros of the closed loop system according to the scheme in Fig. 3 are given as the solutions of the following equations

$$P(s)M(s)S(s) = 0, \tag{21}$$

for $T_{wz}(s)$ given in (15) and

$$Q(s)N(s)S(s) = 0 \tag{22}$$

for $T_{dz}(s)$ given in (16). Obviously the zeros of the shaper appear as the zeros of both the closed loop transfer functions $T_{wz}(s)$ and $T_{dz}(s)$.

The closed loop poles (i.e. the poles of both transfer functions $T_{wz}(s)$ and $T_{dz}(s)$) are given as the solutions of the following characteristic equation

$$CE(s) = S(s)Q(s)N(s) + P(s)M(s) = 0. \tag{23}$$

The following property on the distribution of the spectrum of poles at high magnitudes is crucial with respect to the robustness and stability features of the closed loop system.

Lemma 1: There exists a finite value $c \in \mathbb{R}^+, c >> 0$, such that for large values of magnitudes $|s| > c$, the spectrum of roots of the equation (23) asymptotically approaches the spectrum of zeros of the shaper $S(s)$, given either by (3) for ZV or by (8) for DZV shapers.

Proof Analogously as in [2], let the characteristic equation (23) be transformed to the form

$$CE(s) = S(s)\frac{Q(s)N(s)}{s^{q+n}} + \frac{P(s)M(s)}{s^{q+n}} = 0. \tag{24}$$

As $q+n > p+m$, for $|s| \to \infty$, $\frac{P(s)M(s)}{s^{q+n}} \to 0$ and $\frac{Q(s)N(s)}{s^{q+n}} \to b, b \in \mathbb{R}$. Thus, there exists c such that for $|s| > c$, $\frac{1}{b}S(s)$ is the term in (24) with the predominant order of magnitude and the roots of (24) and (23) tend to match the zeros of $S(s)$ in the given region.□

The above described behavior of closed loop system poles with large magnitudes is especially important when the

inverse ZV shaper is used. Notice that the spectrum of zeros of ZV shaper given by (3) can be located very close to the imaginary axis, especially if the shaper is designed to compensate purely damped oscillatory mode. Regarding the spectrum of zeros of the DZV shaper (8), it has much better features, as it departs from the imaginary axis with increasing moduli of zeros following the asymptotic exponentials [22]. Thus, due to property described above, the application of inverse DZV shaper is much safer compared to ZV. This will be demonstrated in the following examples. Let us remark that the closed loop system with inverse ZV shaper is a neutral system [3], [8], whereas it is a retarded system with more convenient dynamics, if the inverse DZV shaper is used.

V. SIMULATION EXAMPLE

Let particular blocks engaged in the scheme in Fig 3 be respectively

$$G(s) = \frac{1}{s^2 + s}, \tag{25}$$

$$F(s) = \frac{s}{s^2 + 0.6s + 100}, \tag{26}$$

and

$$C(s) = \frac{10s + 10}{0.01s + 1}. \tag{27}$$

The position (i.e. output of $G(s)$) is controlled by the feedback PD controller $C(s)$ which has been tuned to obtain sufficiently fast and well damped responses of the closed feedback system with no shaper considered, as shown in the topmost axis of Fig. 7. First, the results of spectral analysis are shown in Fig. 6. As can be seen, the task of compensating the couple of $F(s)$ poles $r_{1,2} = -0.3 \pm 9.995$ by couple of shaper zeros is fulfilled by both the control schemes with inverse ZV and DZV shapers with the parameters determined as described in Section III. The spectra of poles of closed loop systems tend to match the spectra of the shapers at high frequency range. This aspect has negative consequences

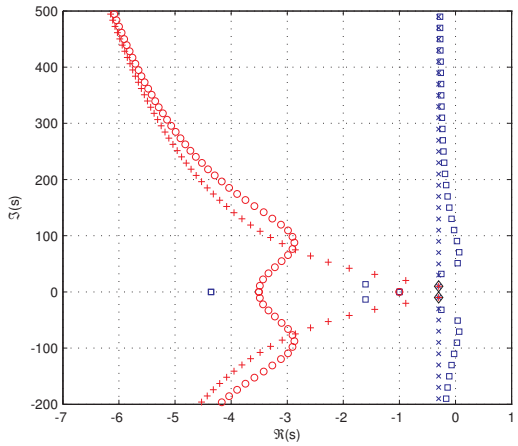

Fig. 6. Simulation example - Spectra: poles $r_{1,2}$ of $F(s)$ to be compensated (black $\diamond$), ZV zeros (blue $\times$), DZV zeros (red $+$), poles of $T_{wz}(s)$ and $T_{dz}(s)$ i) with inverse ZV shaper (blue $\square$), ii) with inverse DZV shaper (red $\circ$)

for the dynamics of the closed loop system with inverse ZV shaper, as there appear three couples of unstable higher frequency poles. On the contrary, the dynamics of the closed loop system with DZV shaper is safely stable.

The comparison of performances of closed loop systems are given in Fig. 7 (with variable z) and Fig. 8 (with variable y), where both the set-point response (starting at time $t = 5$) and disturbance rejection (starting at time $t = 20$) are shown. In comparison with the closed loop without a shaper (topmost axes) and with ZV shaper in serial connection with the controller (second axes from the top), the improved performance in vibration suppression at variable y of the closed loops with inverse shapers is obvious (third and fourth axes from the top). As can be seen in Fig. 8, both the loops with inverse shapers suppress very well the undesirable oscillations in y induced by both the set-point w and the disturbance d changes. Notice that in agreement with above stated theoretical conclusions, the loop with ZV shaper placed between the controller and the system is ineffective in suppressing the oscillations of y induced by the change in the disturbance variable d. From the performance comparison of all the controlled schemes in Fig. 8, the scheme with DZV inverse shaper provides far the best results. Even though the scheme with inverse ZV shaper is fairly efficient in suppressing the undesirable oscillations at the variable y, in agreement with the spectral analysis, its closed loop dynamics is unstable due to high frequency unstable modes. This can be seen in the third axes from the top in both Fig. 7 and Fig. 8.

VI. EXPERIMENTAL VERIFICATION

A. Flexible link setup

The Quanser Inc. laboratory experiment "Flexible Link" was used and tailored, see Fig. 9. A rigid lightweight link (B, $r = 350mm$, the "manipulator arm") was attached to the original rotating table (A), and a flexible beam (C, $L = 350mm$) was mounted at the end of the arm to simulate flexible manipulated load. The angular frequency and damping ratio of the flexible beam first bending mode are respectively $\omega = 8.98rad/s$ and $\zeta = 0.14$. Regarding the rotation table, its angular position is measured by resistance position sensor, and it is actuated by the input DC drive voltage. The plant simplified model transfer function reads

$$G(s) = \frac{z(s)}{u(s)} = \frac{15490}{s^2 + 19s}. \tag{28}$$

The goal is to design a fast control system - positioning servo - that at the same time does not excite the flexible modes of the load. Note that in this setup, the rigid body mechanics can be considered as decoupled from the flexible dynamics, in accordance with Figs. 1 - 3, which is desirable for our intended demonstrations. The experiment is attached to MATLAB/Simulink/Real Time Toolbox [1] by means of dedicated PCI card, and all controllers and shapers are implemented in the MATLAB environment [2], with sampling frequency of 200Hz. The feedback controller (position servo)

[1] www.quanser.com
[2] www.mathworks.com

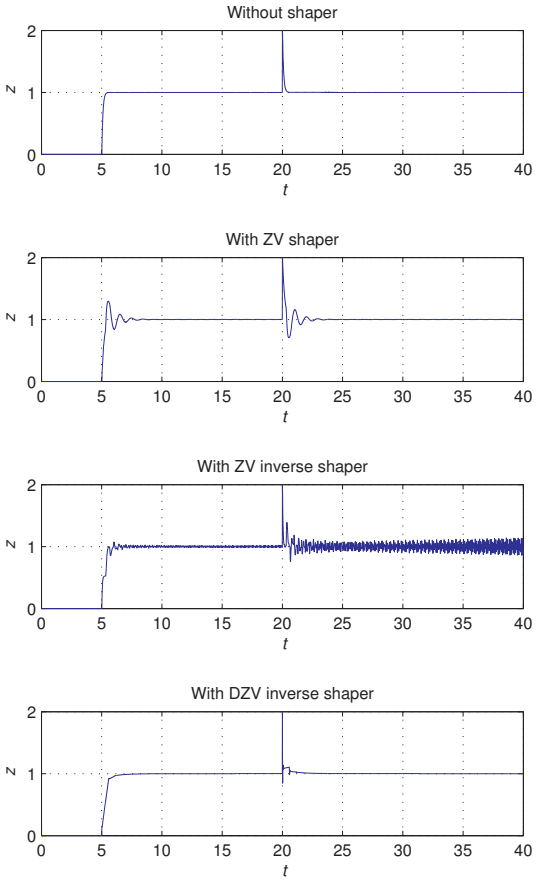

Fig. 7. Simulation example - Set-point responses (starting at time $t = 5$) and disturbance rejections (starting at $t = 20$) of the closed loop system with various control schemes

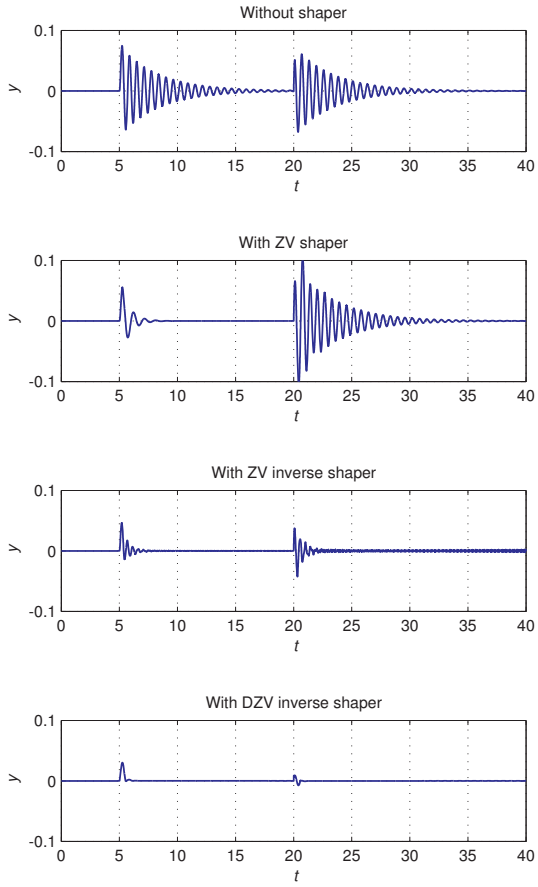

Fig. 8. Simulation example - Responses of the System 2 to the inputs shown in Fig. 7

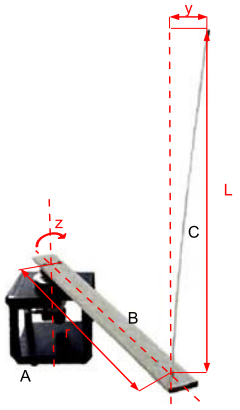

Fig. 9. Flexible link experiment setup.

was designed, with transfer function

$$C(s) = 0.1\frac{s+30}{s+130}, \tag{29}$$

tuned using classical frequency domain techniques (loop-shaping). Resulting closed loop bandwidth is around $20rad/s$ and it is apparently fast enough to excite the flexible beam vibrations unless a dedicated signal shaper is engaged.

B. Measured results

The inverse ZV shaper gives rise to an unstable closed loop in this experiment unsurprisingly. The inverse DZV shaper, on the contrary, with parameters $B = 0.26, \vartheta = 0.57$ works flawlessly.

Measured results[1] for both the reference command tracking and the disturbance rejection are depicted in Fig. 10 and Fig. 11. Particularly, the angular position of the table and the corresponding residual vibrations of the flexible beam are shown for two cases - without a shaper and with the DZV inverse shaper in the feedback loop as in Fig. 3. To emulate the unmeasurable disturbance, the table was manually disturbed from its controlled position and released. Vibrations of the flexible beam excited during the experiments were captured by a video camera and processed off-line using an appropriate video-processing software. Peak to peak points of tip movement were identified and plotted into the graphs.For both the reference command excitations (Fig. 10) and disturbance rejection (Fig. 11), one can appreciate the vibrations reduction achieved by the proposed inverse DZV shaper in the feedback configuration of Fig. 3 compared to the loop with no shaper.

[1] videos available at http://www.cak.fs.cvut.cz/projects/shapers

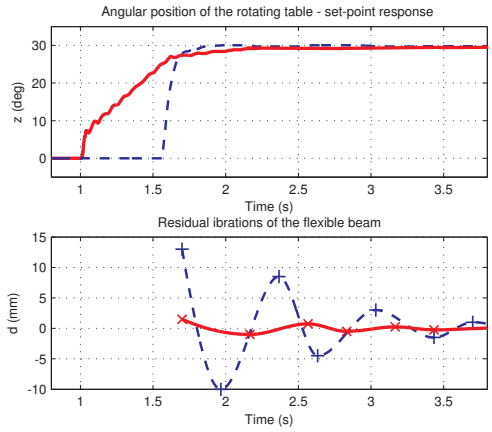

Fig. 10. Measured set-point response of the rotation table and induced residual vibrations of the flexible beam; blue dashed - no shaper (step at $t = 1s$), red solid - inverse DZV shaper in the feedback loop ($t = 1.55s$).

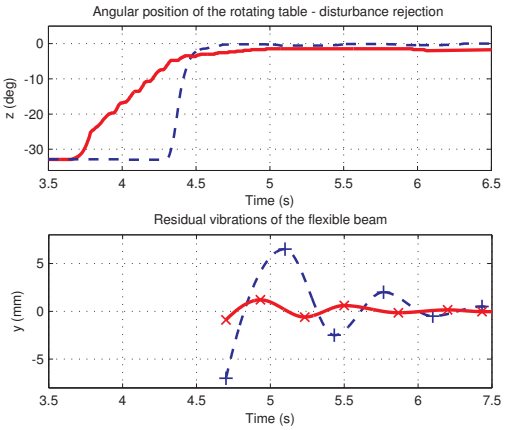

Fig. 11. Measured disturbance rejection of the rotation table and induced residual vibrations of the flexible beam; blue dashed - no shaper, red solid - inverse DZV shaper in the feedback loop. Rotation table manually deflected from the zero position and released at time $t = 3.7s$ for DZV and at time $t = 4.3s$ for the no-shaped cases.

VII. CONCLUSIONS

New feedback control architecture for signal shapers was proposed, which unlike existing solutions addresses both the reference tracking and disturbance attenuation related vibrations problems. The solution is based on inclusion of a shaper inverse dynamics into the feedback loop. Recently introduced DZV shaper appears especially useful in this context because of its higher-damped spectral pattern compared to the traditional ZV lumped-delay counterparts. There is one important open question at this moment regarding systematic design of the feedback controller $C(s)$. Any type of shaper included in the closed loop causes its infinite dimensionality. This aspect needs to be taken into consideration in designing the controller $C(s)$. Next, notice that for small values of parameter B of the inverse DZV shaper (with the limit case $B \to 0$), which corresponds to the low damped (and even undamped) oscillations to be suppressed, the maximum of the inverse DZV shaper magnitude is very large (it goes to infinity for the limit case). This aspect can have negative consequences on the closed loop robustness and will be studied in the subsequent research.

REFERENCES

[1] Baumgart, M.D., Pao, L.Y. (2007). Discrete time-optimal command shaping, *Automatica*, 43, 1403-1409.

[2] Bellman R., Cooke K.L., (1963), *Differential-difference equation*, Academic Press, New York.

[3] Hale, J. K., and Verduyn Lunel, S. M., (1993), *Introduction to functional differential equations,* Vol. 99 of Applied Mathematical Sciences, Springer Verlag New York Inc.

[4] Huey J. R. and Singhose W. (2010), Trends in the Stability Properties of CLSS Controllers: A Root-Locus Analysis, *IEEE Transactions on control system technology*, Vol. 18, No. 5, pp. 1044-1056.

[5] Huey J. R., Sorensen K. L., Singhose W. E. (2008), Useful application of closed-loop signal shaping controllers, *Control Engineering Practice*, Vol. 16, pp. 836-846

[6] Hung J. Y. (2003), Feedback Control With Posicast. *IEEE Transactions on industrial electronics*, Vol. 50, No. 1, pp. 94-99.

[7] Magee, D.P. and W.J. Book, Implementing Modified Command Filtering to Eliminate Multiple Modes of Vibration, Proceedings, *1993 American Control Conference*, San Francisco, CA, June 2-4, 1993, pp 2700-2703.

[8] Michiels, W. and Vyhlídal, T, (2005), An Eigenvalue Based Approach for the Stabilization of Linear Time-Delay Systems of Neutral Type, *Automatica*, Vol. 41, pp. 991-998

[9] Park J., Chang P. H., Park H. S., Lee E.(2006), Design of Learning Input Shaping Technique for Residual Vibration Suppression in an Industrial Robot, *IEEE/ASME Transaction on mechatronics*, Vol. 11, No. 1.

[10] Pereira E., Trapero J.R., Diaz I.M., Feliu V., (2009) Adaptive input shaping for manoeuvring flexible structures using an algebraic identification technique, *Automatica*, Vol. 45, Issue 4, pp. 1046-1051.

[11] Pai M. C.,(2010) Closed-loop input shaping control of vibration in flexible structures using discrete-time sliding mode,. *J. Robust. Nonlinear Control*, Publicated online in Wiley InterScience,

[12] Smith, O.J.M (1957), Posicast control of damped oscillatory systems, *Proceedings of the IRE col 45*, September 1957, pp 1249-1255.

[13] Smith O.J.M., Feedback Control Systems. New York: McGraw-Hill Book Co., Inc., 1958.

[14] Gimpel D.J. and Calvert J. F. (1952), Signal Component Control, *AIEE Transactions*, pp. 339-343, 1952.

[15] Singer, N.C. a Seering, W.P. (1990), Preshaping command input to reduce system vibration, *Journal of Dynamics, System, Measure and Control*, vol 112., pp 76-82.

[16] Singhose W. E., Seering W., Singer N. C., (1994),Residual vibration reduction using vector diagrams to generace shaped inputs, *Journal of Mechanical Design*. 1994, 116: 654-659

[17] Singhose W.E., Sung Y.G. (2009), Robustness analysis of input shaping commands for two-modes flexible systems, *IET Control Theory and Applications*, 2009, Vol. 3, Iss. 6, pp. 722-730

[18] Staehlin U. and Singh T. (2003), Design of closed-loop input shaping controllers, in *American Control Conference*, Denver, Co, 2003, pp. 51675172.

[19] Ragunathan S., Frakes D., Peng K., Singhose W.(2011), Filtering effects on input-shaped command signals for effective crane control, *International Conference on Control and Automation (ICCA)*, Santiago,Chile,19-21 December

[20] Tuttle, T.D., Seering, W.P, A zero-placement technique for designing shaped inputs to suppress multiple-mode vibration, American Control Conference, 1994, Vol. 3, pp 2533-2537.

[21] Vaughan J., Yano A., Singhose W., (2008), Comparison of robust input shapers, *Journal of Sound and Vibration*, Vol. 315,pp. 797815.

[22] Vyhlídal, T. and Zítek, P. (2009), Mapping based algorithm for large-scale computation of quasi-polynomial zeros, *IEEE Transactions on Automatic Control*, Vol. 54, No. 1, pp. 171-177.

[23] T. Vyhlidal, V. Kucera, M. Hromcik. Input shapers with uniformly distributed delays. 10^{th} *IFAC Workshop in Time Delay Systems*, Boston, June 22-44, 2012.

[24] Vyhlidal T., Kucera V., Hromcik M (2012) Signal shapers with distributed delays: spectral analysis and design, Submitted to Automatica

[25] Yi S., Nelson P. W. and Ulsoy A. G.(2010), Time-Delay Systems: Analysis and Control Using the Lambert W Function, Imperial College Press, 2010.